Nonlinear Dyn (2023) 111:10393–10405
https://doi.org/10.1007/s11071-023-08366-1

ORIGINAL PAPER

Soliton, breather, rogue wave and continuum limit for the spatial discrete Hirota equation by Darboux–Bäcklund transformation

Fang-Cheng Fan · Zhi-Guo Xu · Shao-Yun Shi

Received: 26 December 2022 / Accepted: 18 February 2023 / Published online: 20 March 2023

Abstract In this paper, the spatial discrete Hirota equation is investigated by Darboux–Bäcklund transformation. Firstly, the pseudopotential of the spatial discrete Hirota equation is proposed for the first time, from which a Darboux–Bäcklund transformation is constructed. Comparing it with the corresponding one-fold Darboux transformation, we find that they are equivalent because there is no difference except for a constant times. We believe that this equivalence may hold universal if these two transformations are all derived from the same discrete spectral problem and using the similar technique in the references. Secondly, starting from vanishing and plane wave backgrounds, a variety of nonlinear wave solutions, including bell-shaped one-soliton, three types of breathers, W-shaped soliton, periodic solution and rogue wave are given, and the relevant dynamical properties and evolutions are illustrated by plotting figures. The relationship between parameters and solutions' structures is studied in detail, and the related method and technique can also be extended to other nonlinear integrable equations. Finally, we show that the continuum limit of breather and rogue wave solutions of the spatial discrete Hirota equation yields the counterparts of the Hirota equation. The results in this paper might be useful for understanding some physical phenomena in nonlinear optics.

Keywords Spatial discrete Hirota equation · Darboux–Bäcklund transformation · Soliton · Breather · Rogue wave · Continuum limit

Z. Xu (✉)
School of Mathematics, Jilin University, Changchun 130012, People's Republic of China
e-mail: xuzg2014@jlu.edu.cn

F. Fan
School of Mathematics and Statistics, Minnan Normal University, Zhangzhou 363000, People's Republic of China

F. Fan
School of Mathematical Sciences, Shanghai Jiao Tong University, Shanghai 2002240, People's Republic of China

S. Shi
School of Mathematics, Jilin University, Changchun 130012, People's Republic of China

S. Shi
State Key Laboratory of Automotive Simulation and Control, Jilin University, Changchun 130012, People's Republic of China

1 Introduction

The Hirota equation introduced in [1] has the form:

$$i\nu_\tau = \gamma(\nu_{xx} + 2|\nu|^2\nu) + \mathrm{i}\alpha(\nu_{xxx} + 6|\nu|^2\nu_x), \tag{1}$$

where the complex function $\nu = \nu(x, \tau)$ denotes the wave envelopes, the subscripts represent partial differentiation to τ and x, the parameters γ and α are real positive constants and $i = \sqrt{-1}$ stands for imaginary unit. Equation (1) is a typical integrable system in soliton theory and it has attracted a great deal of attention because of its physical applications in the vortex motion and the nonlinear optics [2]. For Eq. (1), the inverse scattering transform and Darboux transformation were performed and N-soliton solutions, rogue wave solutions and gauge equivalence were generated and systematically studied [3–7]. By means of the Ablowitz–Ladik's formulation, Porsezian and Lakshmanan [8] constructed the integrable semi-discrete Hirota equation

$$\begin{aligned} \mathrm{i}u_{n,t} &= \gamma(u_{n+1} - 2u_n + u_{n-1} + |u_n|^2(u_{n+1} + u_{n-1})) \\ &\quad + \mathrm{i}\alpha((1 + |u_n|^2)(u_{n+1} - u_{n-1})), \end{aligned} \tag{2}$$

which yields to the Hirota equation (1) in the continuum limit and can be regarded as an integrable semi-discretizations of Eq. (1). Many excellent and meaningful results related to Eq. (2) have been obtained. For instance, bright and dark soliton solutions were generated based on the Hirota bilinear method [9,10] and Darboux transformation [11], and rogue waves were given in [12,13]. However, one can check that these discrete solutions of the semi-discrete Hirota equation (2) does not converge to the solutions of the Hirota equation (1). Because of this reason, the following spatial discrete Hirota equation was proposed and investigated [14]

$$\begin{aligned} u_{n,t} &= \alpha(1 + |u_n|^2)[u_{n+2} - u_{n-2} + 2u_{n-1} - 2u_{n+1} \\ &\quad + u_n^*(u_{n+1}^2 - u_{n-1}^2) - |u_{n-1}|^2 u_{n-2} + |u_{n+1}|^2 u_{n+2} \\ &\quad + u_n(u_{n-1}^* u_{n+1} - u_{n+1}^* u_{n-1})] \\ &\quad - \beta i(1 + |u_n|^2)(u_{n+1} + u_{n-1}) + 2\beta i u_n, \end{aligned} \tag{3}$$

where $u_n = u(n,t)$ is a complex-valued function of discrete space variable n and time variable t, $u_{n,t} = \frac{\mathrm{d}}{\mathrm{d}t}u_n$ and $*$ denotes the complex conjugate. In [14], the authors showed that the Lax pair, Darboux transformation and soliton solutions for the spatial discrete Hirota equation (3) yield to the corresponding results for the Hirota equation (1). The higher-order rogue wave solutions, which display triangular patterns and pentagons with different peaks, were investigated in [15]. By the Darboux transformation method, the positon solutions and breather solutions of equation (3) were constructed in [16]. Interestingly, the new Lax pair of the spatial discrete Hirota equation (3) was proposed in [17], from which the Darboux transformation, soliton solution, rogue wave solution, breather solution, the continuous limits and gauge equivalent structure were studied.

To describe and understand the physical phenomena simulated by the discrete integrable equations, it is significant to obtain and investigate their explicit exact solutions, especially soliton, breather and rogue wave solutions. Several effective and skillful methods for constructing explicit solutions have been proposed and developed, such as the inverse scattering method [18], the Hirota method [19–21], the algebra-geometric method [22], the discrete Jacobi sub-equation method [23], the Darboux transformation [24–32] and the Darboux–Bäcklund transformation [33–35]. Among these existing methods, the Darboux–Bäcklund transformation has turned out to be one of efficient skills to obtain soliton solutions. Recently, the pseudopotential of the Ablowitz–Ladik lattice and semi-discrete Hirota equation (2) were proposed, from which the Darboux–Bäcklund transformation of the equations were established and various localized nonlinear wave solutions were given [36,37]. Pseudopotential is an another effective technique to construct the Darboux–Bäcklund transformation, compared with the Darboux transformation, it can avoid complex matrix calculations for us.

To the best of our knowledge, the Darboux–Bäcklund transformation based on the pseudopotential for the spatial discrete Hirota equation (3) has not been reported before; the relationship between parameters and solutions' structures in Eq. (3) has not been investigated due to its complexity; the continuum limit of breather solution and rogue wave solution of equation (3) corresponding to the Lax pair (4) have not been studied. These three aspects are what we focus in this paper. The rest of this paper is organized as follows. In Sect. 2, the Darboux–Bäcklund transformation is constructed by using the pseudopotential, and the comparison between it and the one-fold Darboux transformation is performed. In Sect. 3, various types of nonlinear wave solutions are given and the relationship between parameters and solutions' structures is discussed in detail. In Sect. 4, the continuum limit of breather solution and rogue wave solution related to the Lax pair (4) is investigated. Some remarks and summary are presented in the last section.

2 Darboux–Bäcklund transformation of the spatial discrete Hirota equation

In this section, we will focus on the Darboux–Bäcklund transformation for the spatial discrete Hirota equation (3). From Ref. [14], we know the Lax pair of the spatial discrete Hirota equation (3) is given by

$$E\phi_n = U_n\phi_n, \qquad \phi_{n,t} = V_n\phi_n, \tag{4}$$

where E is the shift operator defined by $E\phi_n = \phi_{n+1}$, $\phi_n = (\phi_{n,1}, \phi_{n,2})^{\mathrm{T}}$ is vector eigenfunction, T denotes the transpose of the vector or matrix and $\lambda \in \mathbb{C}$ stands for the spectral parameter which is independent on the time t. The matrices U_n and V_n have the following forms:

$$U_n = \begin{pmatrix} \lambda & u_n \\ -u_n^* & \lambda^{-1} \end{pmatrix},$$

$$V_n = \alpha \begin{pmatrix} A_n(\lambda, \lambda^{-1}, u_n) & B_n(\lambda, \lambda^{-1}, u_n) \\ -B_n(\lambda^{-1}, \lambda, u_n^*) & A_n(\lambda^{-1}, \lambda, u_n^*) \end{pmatrix} + \beta i \begin{pmatrix} C_n(\lambda, \lambda^{-1}, u_n) & D_n(\lambda, \lambda^{-1}, u_n) \\ D_n(\lambda^{-1}, \lambda, u_n^*) & -C_n(\lambda^{-1}, \lambda, u_n^*) \end{pmatrix},$$

where

$$\begin{aligned} A_n(\lambda, \lambda^{-1}, u_n) &= \frac{1}{2}(\lambda^4 - \lambda^{-4}) \\ &- \lambda^2 + \lambda^{-2} + \lambda^2 u_n u_{n-1}^* \\ &- \lambda^{-2} u_{n-1} u_n^* - 2u_n u_{n-1}^* + (u_n u_{n-1}^*)^2 \\ &+ (1 + |u_{n-1}|^2) u_n u_{n-2}^* + (1 + |u_n|^2) u_{n+1} u_{n-1}^*, \\ B_n(\lambda, \lambda^{-1}, u_n) &= \lambda^3 u_n + \lambda^{-3} u_{n-1} \\ &+ \lambda^{-1}[(1 + |u_{n-1}|^2) u_{n-2} + u_{n-1}^2 u_n^* - 2u_{n-1}], \\ C_n(\lambda, \lambda^{-1}, u_n) &= -u_n u_{n-1}^* - \frac{1}{2}(\lambda - \lambda^{-1})^2, \\ D_n(\lambda, \lambda^{-1}, u_n) &= -u_n \lambda + u_{n-1} \lambda^{-1}. \end{aligned}$$

One can directly verify that the discrete zero curvature condition $U_{n,t} = V_{n+1} U_n - U_n V_n$ of the Lax pair (4) gives rise to the spatial discrete Hirota equation (3).

To construct the Darboux–Bäcklund transformation for the spatial discrete Hirota equation (3), we introduce the variable

$$\Gamma_n = \frac{\phi_{n,1}}{\phi_{n,2}}, \tag{5}$$

which is called as the pseudopotential of equation (3). Using (4), we obtain

$$\begin{aligned} \Gamma_{n+1} &= \frac{\lambda(u_n + \lambda \Gamma_n)}{1 - \lambda u_n^* \Gamma_n}, \\ \Gamma_{n,t} &= -A_n \Gamma_n^2 + B_n \Gamma_n + C_n, \end{aligned} \tag{6}$$

where

$$\begin{aligned} A_n &= -\alpha B_n(\lambda^{-1}, \lambda, u_n^*) + \beta i D_n(\lambda^{-1}, \lambda, u_n^*), \\ C_n &= \alpha B_n(\lambda, \lambda^{-1}, u_n) + \beta i D_n(\lambda, \lambda^{-1}, u_n), \\ B_n &= \alpha \left(A_n(\lambda, \lambda^{-1}, u_n) - A_n(\lambda^{-1}, \lambda, u_n^*) \right) \\ &+ \beta i \left(C_n(\lambda, \lambda^{-1}, u_n) + C_n(\lambda^{-1}, \lambda, u_n^*) \right). \end{aligned}$$

Taking the conjugate of both sides of the first equation in (6) and solving the equations related to u_n and u_n^*, we get

$$u_n = \frac{\lambda \lambda^{*2} \Gamma_n \Gamma_n^* \Gamma_{n+1} - \lambda \Gamma_n \Gamma_{n+1} \Gamma_{n+1}^* + \lambda^* \Gamma_{n+1} - \lambda^2 \lambda^* \Gamma_n}{\lambda \lambda^* (1 - \Gamma_n \Gamma_n^* \Gamma_{n+1} \Gamma_{n+1}^*)}. \tag{7}$$

Inserting (7) into the second equation of (6), through a complicated computation, we derive a equation which is made up of $\Gamma_{n-2}, \Gamma_{n-1}, \Gamma_n, \Gamma_{n+1}, \Gamma_{n+2}$ and λ without variables $u_{n-2}, u_{n-1}, u_n, u_{n+1}$, this equation is so tedious that we omit it for brevity. With the help of Maple, we can verify that this equation is invariant under the transformations of $\Gamma_{n-2} \to \Gamma_{n-2}, \Gamma_{n-1} \to \Gamma_{n-1}, \Gamma_n \to \Gamma_n, \Gamma_{n+1} \to \Gamma_{n+1}, \Gamma_{n+2} \to \Gamma_{n+2}, \lambda \to \lambda^{*-1}$. In other words, there exists new variable $\tilde{u}_n$ satisfying the same form of Eqs. (6) when $\lambda \to \lambda^{*-1}$, in which $\tilde{u}_n$ is considered as the new solution of equation (3). From the first equation of (6) and (7), using the transformation $\lambda \to \lambda^{*-1}$, the relation between the old solution u_n and new solution $\tilde{u}_n$ can be derived as

$$\tilde{u}_n = \frac{\lambda \lambda^* + \Gamma_n \Gamma_n^*}{1 + \lambda \lambda^* \Gamma_n \Gamma_n^*} u_n + \frac{(\lambda^2 \lambda^{*2} - 1) \Gamma_n}{\lambda^* (1 + \lambda \lambda^* \Gamma_n \Gamma_n^*)}. \tag{8}$$

which is called as the Darboux–Bäcklund transformation of Eq. (3). Based on (8), we can iterate the old solutions u_n to get new ones $\tilde{u}_n$. It should be remarked that if the resulting solution is taken as the new starting point, and use the Darboux–Bäcklund transformation (8) once again, then another new solutions of equation (3) can be obtained. This process can be done continuously. Therefore, we can generate a sequence of explicit solutions for the spatial discrete Hirota equation (3).

In [14], by means of the Lax pair (4), the one-fold Darboux transformation related to Eq. (3) was given

$$\tilde{u}_n = \frac{\lambda}{\lambda^*} \left(\frac{\lambda \lambda^* + \Gamma_n \Gamma_n^*}{1 + \lambda \lambda^* \Gamma_n \Gamma_n^*} u_n + \frac{(\lambda^2 \lambda^{*2} - 1) \Gamma_n}{\lambda^* (1 + \lambda \lambda^* \Gamma_n \Gamma_n^*)} \right). \tag{9}$$

Comparing the transformation (8) with (9), we find there is no difference except for a constant times. Noticing $\left| \frac{\lambda}{\lambda^*} \right| = 1$, so we consider these two transformations are equivalent. Moreover, we believe the equivalence may hold universal if the two transformations are all derived from the same discrete spectral problem and using the similar methods and techniques employed in literatures [36,37] and [14,38], respectively. To illustrate this fact, we establish the Darboux–Bäcklund transformation of the generalized discrete Hirota equation studied in [13] and the discrete complex mKdV equation proposed in [39]. Comparing with the one-fold Darboux transformations obtained in [13,39], we observe that they remain equivalent.

In [17], by using the other new Lax pair, the one-fold Darboux transformation related to Eq. (3) was derived

$$\tilde{u}_n = \frac{\lambda^2(1+\Gamma_n\Gamma_n^*)}{1+\lambda^2\lambda^{*2}\Gamma_n\Gamma_n^*}u_n + \frac{\lambda^2(\lambda^2\lambda^{*2}-1)\Gamma_n}{\lambda^{*2}(1+\lambda^2\lambda^{*2}\Gamma_n\Gamma_n^*)},$$

which is not equivalent with the transformation (8). Therefore, the explicit solutions we obtain in this paper may be different from the ones given in [17].

Although the transformations (8) and (9) are equivalent, the relationship between parameters and solutions' structures in Eq. (3) has not been studied due to its complexity. On the other hand, the continuum limit of the breather and rogue wave solutions of Eq. (3) corresponding to the Lax pair (4) has not been reported before. These two parts are what we focus on in the following two sections.

3 Soliton, breather and rogue wave of the spatial discrete Hirota equation

In this section, we are going to give soliton, breather and rogue wave for the spatial discrete Hirota equation (3) by using the obtained Darboux–Bäcklund transformation (8) from vanishing and plane wave backgrounds, respectively. To figure out the different collision process of solitary waves and the corresponding dynamical properties, we assume that n is a continuous variable from $-\infty$ to $+\infty$ when we plot figures.

3.1 Soliton

Substituting the trivial solution $u_n = 0$ into the Lax pair (4) and solving the related spectral equation, we obtain

$$\phi_{n,1} = \lambda^n e^{\chi(\lambda)t}, \qquad \phi_{n,2} = \lambda^{-n} e^{-\chi(\lambda)t}, \tag{10}$$

where $\chi(\lambda) = \alpha(\frac{1}{2}(\lambda^4-\lambda^{-4})+\lambda^{-2}-\lambda^2) - \frac{1}{2}\beta\mathrm{i}(\lambda-\lambda^{-1})^2$. Let $\lambda = e^{a+ib}$, where a, b are real constants. Then we rewrite (10) as

$$\phi_{n,1} = e^{Z_R+\mathrm{i}Z_I}, \qquad \phi_{n,2} = e^{-Z_R-\mathrm{i}Z_I}, \tag{11}$$

where Z_R and Z_I are the associate real and imaginary parts and given by

$$\begin{aligned} Z_R &= an + \{\alpha[\cos(4b)\sinh(4a) - 2\cos(2b)\sinh(2a)] \\ &\quad + \beta[\sin(2b)\sinh(2a)]\}t, \\ Z_I &= bn + \{\alpha[\sin(4b)\cosh(4a) - 2\sin(2b)\cosh(2a)] \\ &\quad - \beta[\cos(2b)\cosh(2a)] + \beta\}t. \end{aligned}$$

From (11), the pseudopotential (5) of the spatial discrete Hirota equation (3) is derived as

$$\Gamma_n = e^{2Z_R+2\mathrm{i}Z_I}. \tag{12}$$

Thus, by using the Darboux–Bäcklund transformation (8) with (12), a one-soliton solution of the spatial discrete Hirota equation (3) is obtained

$$\tilde{u}_n = \frac{\lambda(|\lambda|^2-|\lambda|^{-2})e^{2\mathrm{i}Z_I}}{2|\lambda|}\operatorname{sech}(2Z_R+\ln|\lambda|). \tag{13}$$

The solution (13) is the same as one obtained in [14], except for the amplitude. However, we mainly pay attention to some physical quantities related to solution (13) and investigate the relationship between the structure of solution (13) and the parameters α, β, λ. From (13), some important physical quantities such as amplitude, width, wave number, velocity, primary phase and energy are listed in Table 1, in which the energy of $|\tilde{u}_n|$ is defined by $E_{|\tilde{u}_n|} = \int_{-\infty}^{+\infty}|\tilde{u}_n|^2 dn$. Based on the Table 1, we find these physical quantities are invariant once the parameters are determined, which means the shape, amplitude, wave-length and direction of the solution $|\tilde{u}_n|$ don't change during the propagation and it is much stable. It is easily seen that this one-soliton solution $|\tilde{u}_n|$ of (13) is nonsingular and displays the evolution structure of bell-shaped one-soliton for arbitrary parameters α, β, λ ($\lambda \neq 0, \pm1, \pm\mathrm{i}$). When the parameters $\alpha = 0.3$, $\beta = 0.2$, $\lambda = 0.2 + 0.8\mathrm{i}$, the corresponding evolution plots are shown in Fig. 1, from which we know that $|\tilde{u}_n|$ admits bell-shaped one-soliton structure and its shape and amplitude keep invariant during the propagation.

3.2 Breather

Three types of breathers, W-shaped soliton and periodic solution to the spatial discrete Hirota equation (3) based on the Darboux–Bäcklund transformation (8) will be presented in this subsection. For this purpose, take a nonzero seed solution-plane wave solution

$$u_n = ce^{\mathrm{i}z_n}, \tag{14}$$

where c is a real-valued constant and called as the amplitude of the plane wave, $z_n = kn + \omega t$, k is wave number and ω is dispersion relation read as $\omega = 2\beta - 2\beta(1+c^2)\cos(k) + 4\alpha(1+c^2)[(3c^2+1)\cos(k) - 1]\sin(k)$. For the plane wave solution (14)

Table 1 Physical quantities of one-soliton solution $|\tilde{u}_n|$ in (13)

Soliton	Amplitude	Width	Wave number	Velocity	Primary phase	Energy
$\lvert\tilde{u}_n\rvert$	$\left\lvert\frac{\lambda(\lvert\lambda\rvert^2-\lvert\lambda\rvert^{-2})}{2\lvert\lambda\rvert}\right\rvert$	$\frac{1}{2a}$	$2a$	$\frac{\nu}{2a}$	$\ln\lvert\lambda\rvert$	$\left\lvert\frac{\lambda^2(\lvert\lambda\rvert^2-\lvert\lambda\rvert^{-2})^2}{8\lvert\lambda\rvert^2 a}\right\rvert$

$\nu=\alpha[\cos(4b)\sinh(4a)-2\cos(2b)\sinh(2a)]+\beta[\sin(2b)\sinh(2a)]$

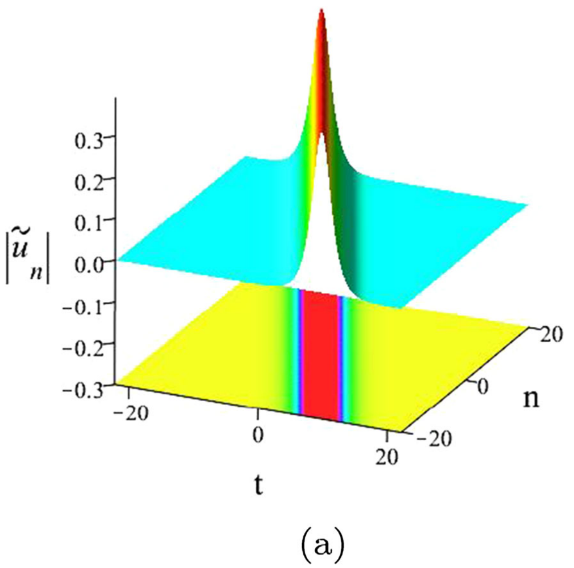

Fig. 1 **a** Bell-shaped one-soliton $|\tilde{u}_n|$ in (13) with parameters $\alpha=0.3$, $\beta=0.2$, $\lambda=0.2+0.8\mathrm{i}$

related to the Lax pair (4), breather and rogue wave solutions and their continuum limits for the spatial discrete Hirota equation (3) have not been studied, which is the main content of our study in the following.

For the sake of brevity, we introduce a gauge transformation related to the initial solution (14)

$$\tilde{\phi}_n=T\phi_n=\begin{pmatrix} e^{-\frac{\mathrm{i}}{2}z_n} & 0\\ 0 & e^{\frac{\mathrm{i}}{2}z_n}\end{pmatrix}\phi_n,$$

under this gauge transformation, we map the variable coefficient Lax pair (4) to the constant coefficient Lax pair,

$$E\tilde{\phi}_n=\tilde{U}_n\tilde{\phi}_n,\qquad \tilde{\phi}_{n,t}=\tilde{V}_n\tilde{\phi}_n, \tag{15}$$

where

$$\tilde{U}_n=\begin{pmatrix}\lambda & c\\ -c & \lambda^{-1}\end{pmatrix},$$
$$\tilde{V}_n=\begin{pmatrix}-\frac{\mathrm{i}}{2}\omega+\alpha A_1+\beta\mathrm{i}A_2 & \alpha cA_3+\beta\mathrm{i}cA_4\\ -\alpha cB_3+\beta\mathrm{i}cB_4 & \frac{\mathrm{i}}{2}\omega+\alpha B_1-\beta\mathrm{i}B_2\end{pmatrix},$$

with

$$\begin{aligned}
A_1&=\frac{1}{2}(\lambda^4-\lambda^{-4})-\lambda^2+\lambda^{-2}+(\lambda^2-2)c^2e^{\mathrm{i}k}\\
&\quad-\lambda^{-2}c^2e^{-\mathrm{i}k}+(3c^2+2)c^2e^{2\mathrm{i}k},\\
A_2&=-c^2e^{\mathrm{i}k}-\frac{1}{2}(\lambda-\lambda^{-1})^2,\\
A_3&=\lambda^3+\lambda^{-3}e^{-\mathrm{i}k}+\lambda[(1+2c^2)e^{\mathrm{i}k}-2]\\
&\quad+\lambda^{-1}[(1+2c^2)e^{-2\mathrm{i}k}-2e^{-\mathrm{i}k}],\\
A_4&=-\lambda+\lambda^{-1}e^{-\mathrm{i}k},\\
B_1&=\frac{1}{2}(\lambda^{-4}-\lambda^4)-\lambda^{-2}+\lambda^2\\
&\quad+(\lambda^{-2}-2)c^2e^{-\mathrm{i}k}-\lambda^2c^2e^{\mathrm{i}k}+(3c^2+2)c^2e^{-2\mathrm{i}k},\\
B_2&=-c^2e^{-\mathrm{i}k}-\frac{1}{2}(\lambda-\lambda^{-1})^2,\\
B_3&=\lambda^{-3}+\lambda^3e^{\mathrm{i}k}+\lambda^{-1}[(1+2c^2)e^{-\mathrm{i}k}-2]\\
&\quad+\lambda[(1+2c^2)e^{2\mathrm{i}k}-2e^{\mathrm{i}k}],\quad B_4=-\lambda^{-1}+\lambda e^{\mathrm{i}k}.
\end{aligned}$$

Solving the corresponding spectral equation related to the Lax pair (15), we obtain

$$\tilde{\phi}_n=\begin{pmatrix}\tilde{\phi}_{n,1}\\ \tilde{\phi}_{n,2}\end{pmatrix}=\begin{pmatrix} C_1\tau_1^ne^{\rho_1t}+C_2\tau_2^ne^{\rho_2t}\\ C_1\frac{\tau_1-\lambda}{c}\tau_1^ne^{\rho_1t}+C_2\frac{\tau_2-\lambda}{c}\tau_2^ne^{\rho_2t}\end{pmatrix},$$

where C_1, C_2 are arbitrary constants and

$$\begin{aligned}
\tau_1&=\frac{1}{2}(\lambda+\lambda^{-1}+\sqrt{\lambda^2+\lambda^{-2}-4c^2-2}),\\
\rho_1&=-\frac{\mathrm{i}}{2}\omega+\alpha A_1+\beta\mathrm{i}A_2+(\alpha A_3+\beta\mathrm{i}A_4)(\tau_1-\lambda),\\
\tau_2&=\frac{1}{2}(\lambda+\lambda^{-1}-\sqrt{\lambda^2+\lambda^{-2}-4c^2-2}),\\
\rho_2&=-\frac{\mathrm{i}}{2}\omega+\alpha A_1+\beta\mathrm{i}A_2+(\alpha A_3+\beta\mathrm{i}A_4)(\tau_2-\lambda).
\end{aligned}$$

Then, the general solution of the Lax pair (4) associated with the initial solution (14) can be given by

$$\begin{aligned}
\phi_n&=T^{-1}\tilde{\phi}_n\\
&=\begin{pmatrix}(C_1\tau_1^ne^{\rho_1t}+C_2\tau_2^ne^{\rho_2t})e^{\frac{\mathrm{i}}{2}z_n}\\ (C_1\frac{\tau_1-\lambda}{c}\tau_1^ne^{\rho_1t}+C_2\frac{\tau_2-\lambda}{c}\tau_2^ne^{\rho_2t})e^{-\frac{\mathrm{i}}{2}z_n}\end{pmatrix}.
\end{aligned}\tag{16}$$

With the help of (16), the pseudopotential (5) of the spatial discrete Hirota equation (3) is derived as

$$\Gamma_n=\frac{C_1\tau_1^ne^{\rho_1t}+C_2\tau_2^ne^{\rho_2t}}{C_1\frac{\tau_1-\lambda}{c}\tau_1^ne^{\rho_1t}+C_2\frac{\tau_2-\lambda}{c}\tau_2^ne^{\rho_2t}}e^{\mathrm{i}z_n}. \tag{17}$$

Let

$$\mu_1 = \frac{\tau_1}{\sqrt{c^2+1}}, \quad \mu_2 = \frac{\tau_2}{\sqrt{c^2+1}}, \eta_1 = \frac{\tau_1 - \lambda}{c},$$
$$\eta_2 = \frac{\tau_2 - \lambda}{c}, \quad \varrho = (\alpha A_3 + \beta \mathrm{i} A_4)\sqrt{\lambda^2 + \lambda^{-2} - 4c^2 - 2}.$$

Then, we can equivalently denote (17) as

$$\Gamma_n = \frac{C_1 \mu_1^n e^{\varrho t} + C_2 \mu_2^n e^{-\varrho t}}{C_1 \eta_1 \mu_1^n e^{\varrho t} + C_2 \eta_2 \mu_2^n e^{-\varrho t}} e^{\mathrm{i} z_n}. \tag{18}$$

Since $\mu_1\mu_2 = 1$, $\eta_1\eta_2 = 1$, we rewrite

$$\mu_1 = e^{\kappa_1 + \mathrm{i}\kappa_2}, \qquad \mu_2 = e^{-(\kappa_1 + \mathrm{i}\kappa_2)},$$
$$\eta_1 = e^{\alpha_1 + \mathrm{i}\alpha_2}, \qquad \eta_2 = e^{-(\alpha_1 + \mathrm{i}\alpha_2)}, \qquad \varrho = \omega_1 + \mathrm{i}\omega_2, \tag{19}$$

where κ_i, α_i and ω_i $(i = 1, 2)$ are the corresponding real and imaginary parts, respectively. Noticing that C_1, C_2 in (18) are arbitrary constants, whose roles are only to change the phase of the nonlinear wave. For the sake of simplicity, we choose $C_1 = 1$, $C_2 = -1$. Thus, by (18) and (19), the pseudopotential of the spatial discrete Hirota equation (3) is constructed as

$$\Gamma_n = \frac{e^{\theta_1 + \mathrm{i}\theta_2} - e^{-(\theta_1 + \mathrm{i}\theta_2)}}{e^{\theta_1 + \mathrm{i}\theta_2 + \alpha_1 + \mathrm{i}\alpha_2} - e^{-(\theta_1 + \mathrm{i}\theta_2 + \alpha_1 + \mathrm{i}\alpha_2)}} e^{\mathrm{i} z_n}, \tag{20}$$

where

$$\theta_1 = \kappa_1 n + \omega_1 t, \quad \theta_2 = \kappa_2 n + \omega_2 t.$$

From (20), we have

$$\Gamma_n = \frac{\sinh(\theta_1)\cos(\theta_2) + \mathrm{i}\cosh(\theta_1)\sin(\theta_2)}{\sinh(\theta_1 + \alpha_1)\cos(\theta_2 + \alpha_2) + \mathrm{i}\cosh(\theta_1 + \alpha_1)\sin(\theta_2 + \alpha_2)} e^{\mathrm{i} z_n}, \tag{21}$$

and

$$\Gamma_n \Gamma_n^* = \frac{\cosh(2\theta_1) - \cos(2\theta_2)}{\cosh(2\theta_1 + 2\alpha_1) - \cos(2\theta_2 + 2\alpha_2)}. \tag{22}$$

Therefore, by using the Darboux–Bäcklund transformation (8) with (21) and (22), the nonlinear wave solution of the spatial discrete Hirota equation (3) is given by

$$\tilde{u}_n = \frac{|\lambda|^2 + \frac{\cosh(2\theta_1) - \cos(2\theta_2)}{\cosh(2\theta_1 + 2\alpha_1) - \cos(2\theta_2 + 2\alpha_2)} + \frac{|\lambda|^4 - 1}{c\lambda^*} \frac{\sinh(\theta_1)\cos(\theta_2) + \mathrm{i}\cosh(\theta_1)\sin(\theta_2)}{\sinh(\theta_1 + \alpha_1)\cos(\theta_2 + \alpha_2) + \mathrm{i}\cosh(\theta_1 + \alpha_1)\sin(\theta_2 + \alpha_2)}}{1 + |\lambda|^2 \frac{\cosh(2\theta_1) - \cos(2\theta_2)}{\cosh(2\theta_1 + 2\alpha_1) - \cos(2\theta_2 + 2\alpha_2)}} c e^{\mathrm{i} z_n}. \tag{23}$$

Obviously, the periodicity of the nonlinear wave solution (23) is mainly affected by θ_2. When $\kappa_1 = 0$, $\kappa_2 \neq 0$, θ_1 is independent of space variable n and θ_2 is periodic with respect to n, so solution (23) is periodic in the n direction; while $\omega_1 = 0$, $\omega_2 \neq 0$, θ_1 is independent of time variable t and θ_2 is periodic with respect to t, then solution (23) becomes periodic in the t direction.

By choosing different parameters $\lambda, c, \alpha, \beta$ and k, the distinct wave structures can be obtained from (23). In what follows, we proceed to give three types of breather solutions, W-shaped soliton solution and periodic solution for the spatial discrete Hirota equation (3) and illustrate their dynamical properties and propagation process by plotting figures. Meanwhile, the relationship between parameters and breathers' structures will be studied in detail.

Firstly, we will investigate the case where λ is real. We are going to discuss solution (23) for two cases under the condition $\lambda^2 + \lambda^{-2} - 4c^2 - 2 \neq 0$, the case of $\lambda^2 + \lambda^{-2} - 4c^2 - 2 = 0$ will be discussed in the next subsection. For the sake of convenience, we define the four sets related to the real parameters c, α, β and k:

$$\Theta_1 = \Big\{\lambda \in \mathbb{R} : \lambda < -c - \sqrt{c^2+1},$$
$$c - \sqrt{c^2+1} < \lambda < -c + \sqrt{c^2+1}, \lambda > c + \sqrt{c^2+1}\Big\},$$
$$\Delta_1 = \Big\{\lambda \in \mathbb{R} : \alpha[\lambda(\lambda^2 - 2) + \lambda^{-1}\cos(k)(\lambda^{-2} - 2)$$
$$+ (1+2c^2)(\lambda\cos(k) + \lambda^{-1}\cos(2k))] + \beta\lambda^{-1}\sin(k) = 0\Big\},$$
$$\Theta_2 = \Big\{\lambda \in \mathbb{R} : -c - \sqrt{c^2+1} < \lambda < c - \sqrt{c^2+1},$$
$$-c + \sqrt{c^2+1} < \lambda < c + \sqrt{c^2+1}\Big\},$$
$$\Delta_2 = \Big\{\lambda \in \mathbb{R} : \alpha[-\lambda^{-1}\sin(k)(\lambda^{-2} - 2)$$
$$+ (1+2c^2)(\lambda\sin(k) - \lambda^{-1}\sin(2k))]$$
$$+ \beta(-\lambda + \lambda^{-1}\cos(k)) = 0\Big\}.$$

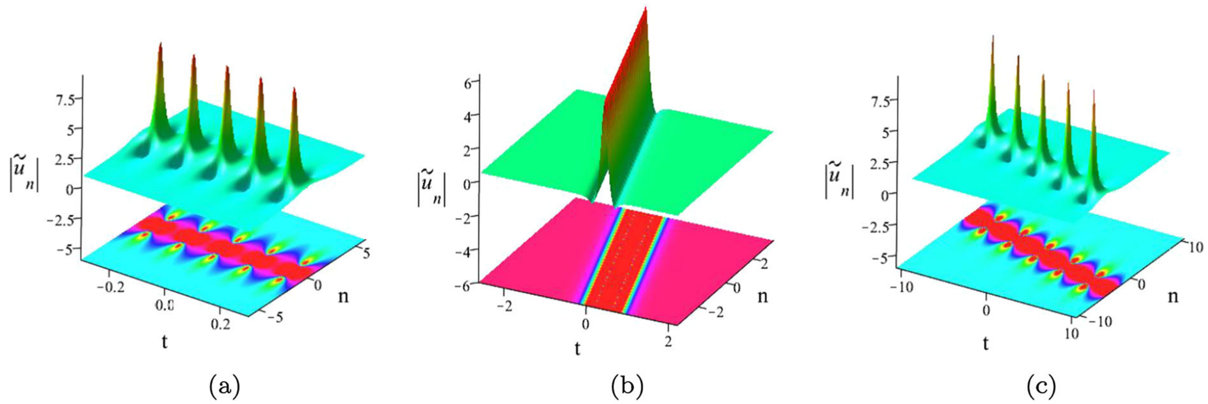

Fig. 2 **a** Time-periodic Kuznetsov–Ma breather $|\tilde{u}_n|$ in (23) with parameters $\lambda = 2.8950$, $c = 0.5$, $\alpha = 0.1$, $\beta = 5.0$, $k = 4.0$; **b** W-shaped soliton $|\tilde{u}_n|$ in (23) with parameters $\lambda = 0.3552$, $c = 0.5$, $\alpha = 0.1$, $\beta = 0.01$, $k = 0.01$; **c** Spatiotemporally periodic breather $|\tilde{u}_n|$ in (23) with parameters $\lambda = 2.8$, $c = 1.0$, $\alpha = 0.01$, $\beta = 0.2$, $k = 2.8$

Table 2 The relationship between parameter λ and solutions' structures in (23)

λ	$\kappa_1, \quad \kappa_2$	$\omega_1, \quad \omega_2$	θ_1	θ_2	$\lvert\tilde{u}_n\rvert$
$\lambda \in \Theta_1 \bigcap \Delta_1$	$\kappa_1 \neq 0,\ \kappa_2 = 0$	$\omega_1 = 0,\ \omega_2 \neq 0$	$\theta_1 = \kappa_1 n$	$\theta_2 = \omega_2 t$	KM
$\lambda \in \Theta_1 \bigcap \Delta_2$	$\kappa_1 \neq 0,\ \kappa_2 = 0$	$\omega_1 \neq 0,\ \omega_2 = 0$	$\theta_1 = \kappa_1 n + \omega_1 t$	$\theta_2 = 0$	WS
$\lambda \in \Theta_1 \cap C_{\mathbb{R}}(\Delta_1 \cup \Delta_2)$	$\kappa_1 \neq 0,\ \kappa_2 = 0$	$\omega_1 \neq 0,\ \omega_2 \neq 0$	$\theta_1 = \kappa_1 n + \omega_1 t$	$\theta_2 = \omega_2 t$	SB

The KM, WS and SB denote the time-periodic Kuznetsov–Ma breather, W-shaped soliton and spatiotemporally periodic breather, respectively

Case 1: $\lambda \in \Theta_1$. For real parameters c, α, β and k, we know that μ_1, μ_2 in (19) are real when $\lambda \in \Theta_1$. Meanwhile, we notice that the expression Γ_n in (18) are the same whether $\mu_1 > 0$, $\mu_2 > 0$ or $\mu_1 < 0$, $\mu_2 < 0$. Without loss of generality, we suppose that $\mu_1 > 0$, $\mu_2 > 0$. Then, we conclude that $\kappa_1 \neq 0$, $\kappa_2 = 0$ when $\lambda \in \Theta_1$. In this case, each component of ϱ in (18) can be split into real and imaginary parts as

$$\varrho = \omega_1 + \mathrm{i}\omega_2,$$

where

$$\begin{aligned}\omega_1 = &\{\alpha[\lambda(\lambda^2 - 2) + \lambda^{-1}\cos(k)(\lambda^{-2} - 2)\\ &+ (1 + 2c^2)(\lambda\cos(k) + \lambda^{-1}\cos(2k))]\\ &+ \beta\lambda^{-1}\sin(k)\}\sqrt{\lambda^2 + \lambda^{-2} - 4c^2 - 2},\\ \omega_2 = &\{\alpha[-\lambda^{-1}\sin(k)(\lambda^{-2} - 2) + (1 + 2c^2)(\lambda\sin(k)\\ &- \lambda^{-1}\sin(2k))] + \beta(-\lambda + \lambda^{-1}\cos(k))\}\\ &\sqrt{\lambda^2 + \lambda^{-2} - 4c^2 - 2}.\end{aligned}$$

When $\lambda \in \Theta_1 \bigcap \Delta_1$, we can verify that $\kappa_1 \neq 0$, $\kappa_2 = 0$, $\omega_1 = 0$, $\omega_2 \neq 0$, that is $\theta_1 = \kappa_1 n$ and $\theta_2 = \omega_2 t$, the nonlinear wave solution (23) is localized in the n direction and periodic in the t direction, which can be considered as the time-periodic Kuznetsov–Ma breather, the amplitude distribution and evolution states corresponding different n under the condition of $\lambda = 2.8950$, $c = 0.5$, $\alpha = 0.1$, $\beta = 5.0$, $k = 4.0$ are illustrated in Fig. 2a. When $\lambda \in \Theta_1 \bigcap \Delta_2$, it is easy to verify that $\kappa_1 \neq 0$, $\kappa_2 = 0$, $\omega_1 \neq 0$, $\omega_2 = 0$, that is $\theta_1 = \kappa_1 n + \omega_1 t$ and $\theta_2 = 0$, the nonlinear wave solution (23) is localized both in the n and t direction, the W-shaped soliton solution can be obtained from (23), the evolution and density contour of this type by choosing parameters $\lambda = 0.3552$, $c = 0.5$, $\alpha = 0.1$, $\beta = 0.01$, $k = 0.01$ are showed in Fig. 2b. When $\lambda \in \Theta_1 \bigcap C_R(\Delta_1 \bigcup \Delta_2)$, we have $\kappa_1 \neq 0$, $\kappa_2 = 0$, $\omega_1 \neq 0$, $\omega_2 \neq 0$, that is $\theta_1 = \kappa_1 n + \omega_1 t$ and $\theta_2 = \omega_2 t$, the nonlinear wave solution (23) is localized both in the n and t direction, we can get the spatiotemporally periodic breather solution from (23), which is displayed in Fig. 2c by choosing parameters $\lambda = 2.8$, $c = 1.0$, $\alpha = 0.01$, $\beta = 0.2$, $k = 2.8$. Comparing with Fig. 2a and c, we can observe the effect of ω_1 to the structure

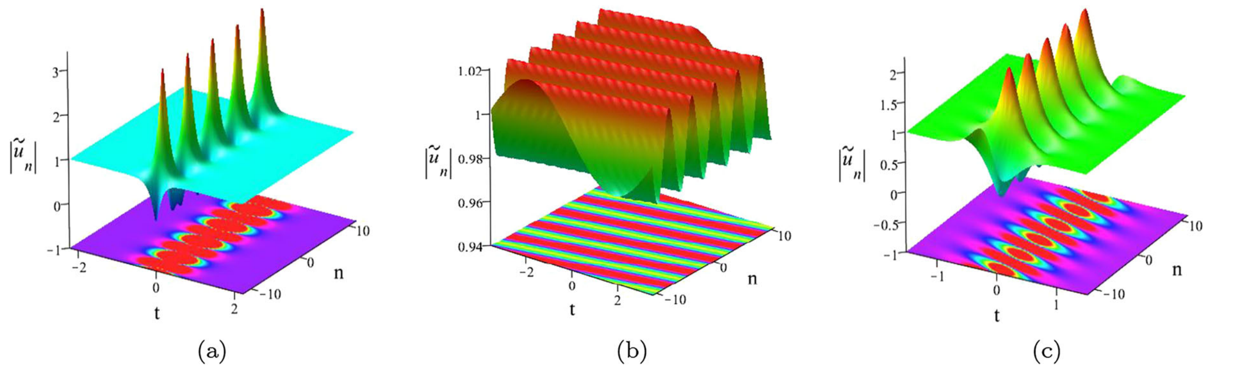

Fig. 3 **a** Space-periodic Akhmediev breather $|\tilde{u}_n|$ in (23) with parameters $\lambda = 1.7238$, $c = 1.0$, $\alpha = 0.1$, $\beta = 1.0$, $k = 3.0$; **b** Periodic solution $|\tilde{u}_n|$ in (23) with parameters $\lambda = 0.9928$, $c = 1.0$, $\alpha = 0.1$, $\beta = 2.0$, $k = 6.0$; **c** Space-periodic Akhmediev breather $|\tilde{u}_n|$ in (23) with parameters $\lambda = 1.4$, $c = 1.0$, $\alpha = 0.1$, $\beta = 1.5$, $k = 1.0$

of breather. From Fig. 2b and c, we can show the effect of ω_2 to the structure of solution. Based on the above facts, we conclude the relationship between parameter λ and solutions' structures as presented in Table 2.

Case 2: $\lambda \in \Theta_2$. For real parameters c, α, β and k, we find that μ_1, μ_2 are imaginary and $|\mu_1| = |\mu_2| = 1$ when $\lambda \in \Theta_2$, so $\kappa_1 = 0$, $\kappa_2 \neq 0$. Meanwhile, each component of ϱ in (18) can be split into real and imaginary parts as

$$\varrho = \omega_1 + \mathrm{i}\omega_2,$$

where

$$\begin{aligned}\omega_1 = &-\{\alpha[-\lambda^{-1}\sin(k)(\lambda^{-2}-2)\\ &+(1+2c^2)(\lambda\sin(k)-\lambda^{-1}\sin(2k))]\\ &+\beta(-\lambda+\lambda^{-1}\cos(k))\}\sqrt{-\lambda^2-\lambda^{-2}+4c^2+2},\\ \omega_2 = &\{\alpha[\lambda(\lambda^2-2)+\lambda^{-1}\cos(k)(\lambda^{-2}-2)\\ &+(1+2c^2)(\lambda\cos(k)+\lambda^{-1}\cos(2k))]\\ &+\beta\lambda^{-1}\sin(k)\}\sqrt{-\lambda^2-\lambda^{-2}+4c^2+2}.\end{aligned}$$

When $\lambda \in \Theta_2 \bigcap \Delta_1$, it is easy to verify that $\kappa_1 = 0$, $\kappa_2 \neq 0, \omega_1 \neq 0, \omega_2 = 0$, that is $\theta_1 = \omega_1 t$ and $\theta_2 = \kappa_2 n$, the nonlinear wave solution (23) is localized in the t direction and periodic in the n direction, which can be regarded as the space-periodic Akhmediev breather, the amplitude distribution and evolution states corresponding different n under the condition of $\lambda = 1.7238$, $c = 1.0$, $\alpha = 0.1$, $\beta = 1.0$, $k = 3.0$ are displayed in Fig. 3a. When $\lambda \in \Theta_2 \bigcap \Delta_2$, we have $\kappa_1 = 0$, $\kappa_2 \neq 0$, $\omega_1 = 0$, $\omega_2 \neq 0$, then $\theta_1 = 0$ and $\theta_2 = \kappa_2 n + \omega_2 t$, the nonlinear wave solution (23) is periodic both in the n and t direction, from (23) we can obtain the periodic solution, which is illustrated in Fig. 3b by choosing parameters $\lambda = 0.9928$, $c = 1.0$, $\alpha = 0.1$, $\beta = 2.0$, $k = 6.0$. When $\lambda \in \Theta_2 \bigcap C_R(\Delta_1 \bigcup \Delta_2)$, we can verify that $\kappa_1 = 0$, $\kappa_2 \neq 0$, $\omega_1 \neq 0$, $\omega_2 \neq 0$, that is $\theta_1 = \omega_1 t$ and $\theta_2 = \kappa_2 n + \omega_2 t$, the nonlinear wave solution (23) is localized in the t direction and periodic in the n direction, the space-periodic Akhmediev breather solution can be obtained from (23), which is displayed in Fig. 3c by choosing parameters $\lambda = 1.4$, $c = 1.0$, $\alpha = 0.1$, $\beta = 1.5$, $k = 1.0$. In this case, we obtain two types of the space-periodic Akhmediev breathers as showed in Fig. 3a and c, respectively, from which we can understand the effect of ω_2 to the structure of breathers. Comparing with Fig. 3b and c, we can show the effect of ω_1 to the structure of solution. Based on the above facts, we conclude the relationship between parameter λ and structures of solutions given in Table 3.

Secondly, we investigate the case where λ is imaginary. In this case, for real parameters c, α, β and k, we are hard to choose appropriate parameters λ so that μ_1, μ_2 and ϱ in (18) can be split into real and imaginary parts as above, which makes it challenging for us to accurately analyse the relationship between parameters and breathers' structures. By experimenting with a large number of parameters, we find that we can only obtain the spatiotemporally periodic breather solutions when λ is imaginary. For instance, when choosing $\lambda = 1.5\mathrm{i}$, $c = 1.0$, $\alpha = 0.4$, $\beta = 0.01$, $k = 0.1$ and $\lambda = 2.0 - 1.2\mathrm{i}$, $c = 1.0$, $\alpha = 0.01$, $\beta = 0.1$, $k = 0.1$,

Table 3 The relationship between parameter λ and solutions' structures in (23)

λ	κ_1, κ_2	ω_1, ω_2	θ_1	θ_2	$\lvert\tilde{u}_n\rvert$
$\lambda \in \Theta_2 \bigcap \Delta_1$	$\kappa_1 = 0,\ \kappa_2 \neq 0$	$\omega_1 \neq 0,\ \omega_2 = 0$	$\theta_1 = \omega_1 t,$	$\theta_2 = \kappa_2 n$	AB
$\lambda \in \Theta_2 \bigcap \Delta_2$	$\kappa_1 = 0,\ \kappa_2 \neq 0$	$\omega_1 = 0,\ \omega_2 \neq 0$	$\theta_1 = 0$	$\theta_2 = \kappa_2 n + \omega_2 t$	PS
$\lambda \in \Theta_2 \cap C_{\mathbb{R}}(\Delta_1 \cup \Delta_2)$	$\kappa_1 = 0,\ \kappa_2 \neq 0$	$\omega_1 \neq 0,\ \omega_2 \neq 0$	$\theta_1 = \omega_1 t$	$\theta_2 = \kappa_2 n + \omega_2 t$	AB

The AB, PS denote the space-periodic Akhmediev breather and periodic solution, respectively

the corresponding spatiotemporally periodic breather solutions are showed in Fig. 4a and b, respectively.

3.3 Rogue wave

The rogue wave solution has the peculiarity of being localized both in the n and t directions and can be constructed from the breather by considering the limit technique in the mathematical point of view. To establish the rogue wave solution for the spatial discrete Hirota equation (3), we take $\lambda^2 + \lambda^{-2} - 4c^2 - 2 = 0$, i.e., $\lambda = \sigma_1 c + \sigma_2\sqrt{c^2+1}$ ($\sigma_1 = \pm 1$, $\sigma_2 = \pm 1$), and choose $C_1 = 1$, $C_2 = -1$ in (17). In this special case, the pseudopotential of the spatial discrete Hirota equation (3) can be derived as

$$\Gamma_n = -\sigma_1 \left(1 + \frac{\sigma_2\sqrt{c^2+1}}{\sigma_1 c n + 2\sigma_1\sigma_2 c\sqrt{c^2+1}\chi t - \sigma_2\sqrt{c^2+1}}\right) e^{i z_n}, \quad (24)$$

where χ is given by replacing λ in $\alpha A_3 + \beta \mathrm{i} A_4$ with $\sigma_1 c + \sigma_2\sqrt{c^2+1}$. For the sake of greater clarity, choosing parameters $\alpha = \frac{1}{10}$, $\beta = 5$, $c = \frac{3}{4}$, $k = 0$, $\sigma_1 = 1, \sigma_2 = 1$ and substituting (24) into the Darboux–Bäcklund transformation (8), the discrete rogue wave solution of the spatial discrete Hirota equation (3) is derived as

$$\tilde{u}_n = -\frac{3}{4}\left(1 + \frac{4608000\mathrm{i}t - 409600}{147456n^2 + 311040nt + 13124025t^2 - 98304n - 103680t + 81920}\right) e^{-\frac{45i}{8}t}, \quad (25)$$

from which we know the maximum value of $|\tilde{u}_n|$ is $\frac{63}{16}$ at the point $(n,t) = (\frac{1}{3}, 0)$, the minimum of $|\tilde{u}_n|$ is always zero and $|\tilde{u}_n| \to \frac{3}{4}$ (background) as $n, t \to \infty$. Thus, we obtain $|\tilde{u}_n|_{max}$=5.25$|\tilde{u}_n|_{n,t\to\infty}$. The profile of the rogue wave solution (25) is showed in Fig. 4c, from which we find it crowds around the point $(n,t) = (\frac{1}{3}, 0)$ and holds one peakon and two depression points, the peak amplitude is at least five times the background. Through a direct calculation, we generate the conservation result $\int_{-\infty}^{+\infty}\left(|\tilde{u}_n|^2 - \frac{9}{16}\right) dn = 0$, which means that the rogue wave is formed from the flat background.

Based on the facts in the Sects. 3.2 and 3.3, we conclude that when $\lambda^2+\lambda^{-2}-4c^2-2 \neq 0$, we are able to obtain the time-periodic Kuznetsov–Ma breather, pace-periodic Akhmediev breather, spatiotemporally periodic breather, W-shaped soliton solution and periodic solution for the spatial discrete Hirota equation (3), while $\lambda^2 + \lambda^{-2} - 4c^2 - 2 = 0$, we can construct the rogue wave solution.

4 Continuum limit of the breather and rogue wave solutions

As we know, the relationship between discrete integrable systems and its relevant continuous counterparts is always quite significant. In [14], the authors showed that the Lax pair, Darboux transformation and soliton solutions of the spatial discrete Hirota equation (3) converge to the corresponding results of the Hirota equation (1). However, the continuum limit of the breather solution and rogue wave solution of Eq. (3) related to the Lax pair (4) has not been investigated, which is what we focus on in this section.

Based on the results in [14], we know the spatial discrete Hirota equation (3) leads to the Hirota equation (1) under the transformation

$$u_n = \delta v(x,\tau), \quad x = n\delta, \quad \tau = 2\delta^3 t, \quad \beta = 2\gamma\delta. \quad (26)$$

For the sake of constructing the continuum limit of the breather solution and rogue wave solution, we define

$$\lambda = e^{\mu\delta} = 1 + \delta\mu + \frac{1}{2}\delta^2\mu^2 + \frac{1}{6}\delta^3\mu^3 + o(\delta^3), \quad (27)$$

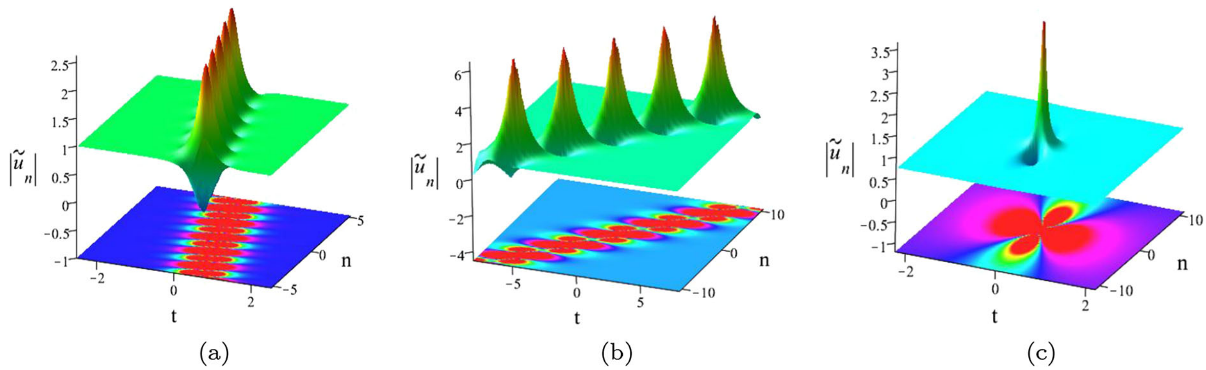

Fig. 4 **a** The spatiotemporally periodic breather $|\tilde{u}_n|$ in (23) with parameters $\lambda = 1.5\mathrm{i}$, $c = 1.0$, $\alpha = 0.4$, $\beta = 0.01$, $k = 0.1$; **b** The spatiotemporally periodic breather $|\tilde{u}_n|$ in (23) with parameters and $\lambda = 2.0 - 1.2\mathrm{i}$, $c = 1.0$, $\alpha = 0.01$, $\beta = 0.1$, $k = 0.1$; **c** The rogue wave $|\tilde{u}_n|$ in (25) with parameters $\alpha = \frac{1}{10}$, $\beta = 5$, $c = \frac{3}{4}$, $k = 0$, $\sigma_1 = 1$, $\sigma_2 = 1$

where μ is a constant spectral parameter. We suppose that the continuum limit of Γ_n is Γ. Then, by a direct analysis of the Darboux–Bäcklund transformation (8), we obtain the relation between $\tilde{u}_n$ and $\tilde{v}$:

$$\tilde{u}_n = \delta \tilde{v} + o(\delta), \tag{28}$$

where

$$\Gamma = \frac{e^{r_1 x + [(\alpha(4\mu^2 - \mathfrak{k}^2 + 2\mathfrak{c}^2) + \gamma \mathfrak{k}) + 2\mathrm{i}\mu(\alpha \mathfrak{k} - \gamma)] r_1 \tau} - e^{r_2 x + [(\alpha(4\mu^2 - \mathfrak{k}^2 + 2\mathfrak{c}^2) + \gamma \mathfrak{k}) + 2\mathrm{i}\mu(\alpha \mathfrak{k} - \gamma)] r_2 \tau}}{\frac{r_1 - \mu}{\mathfrak{c}} e^{r_1 x + [(\alpha(4\mu^2 - \mathfrak{k}^2 + 2\mathfrak{c}^2) + \gamma \mathfrak{k}) + 2\mathrm{i}\mu(\alpha \mathfrak{k} - \gamma)] r_1 \tau} - \frac{r_2 - \mu}{\mathfrak{c}} e^{r_2 x + [(\alpha(4\mu^2 - \mathfrak{k}^2 + 2\mathfrak{c}^2) + \gamma \mathfrak{k}) + 2\mathrm{i}\mu(\alpha \mathfrak{k} - \gamma)] r_2 \tau}} e^{\mathrm{i}(\mathfrak{k} x + \omega \tau)}, \tag{33}$$

$$\tilde{v} = v + \frac{2(\mu + \mu^*)\Gamma}{1 + \Gamma \Gamma^*},$$

which is nothing but the one-fold Darboux transformation of the Hirota equation (1) given in [40].

In what follows, we are going to construct the continuum limit of the breather solution (23). Setting

$$c = \mathfrak{c}\delta, \quad k = \mathfrak{k}\delta, \tag{29}$$

where $\mathfrak{c}$ and $\mathfrak{k}$ are real constants. Then, the leading term of the plane wave solution (14) is given

$$v = \mathfrak{c} e^{\mathrm{i}(\mathfrak{k} x + \omega \tau)}, \quad \omega = \gamma(\mathfrak{k}^2 - 2\mathfrak{c}^2) + \alpha \mathfrak{k}(6\mathfrak{c}^2 - \mathfrak{k}^2) \tag{30}$$

which is just a plane wave solution of the Hirota equation (1). Notice that τ_j $(j = 1, 2)$ in (16) admits the equation

$$\tau_j^2 - (\lambda + \lambda^{-1})\tau_j + c^2 + 1 = 0. \tag{31}$$

Let $\tau_j = e^{r_j \delta}$ and using (27) and (29), the leading term of characteristic Eq. (31) yields continuous counterpart

$$r_j^2 - \mu^2 + \mathfrak{c}^2 = 0. \tag{32}$$

Choosing $C_1 = 1$, $C_2 = -1$ in (17) and using (26), (27) and (29), we construct the continuum limit of Γ_n as

where r_1, r_2 are obtained from (32), i.e. $r_1 = \sqrt{\mu^2 - \mathfrak{c}^2}$ and $r_2 = -\sqrt{\mu^2 - \mathfrak{c}^2}$. We can verify $\frac{r_1 - \mu}{\mathfrak{c}} \frac{r_2 - \mu}{\mathfrak{c}} = 1$, so we define $\frac{r_1 - \mu}{\mathfrak{c}} = e^{\alpha_2 + \mathrm{i}\beta_2}$, $\frac{r_2 - \mu}{\mathfrak{c}} = e^{-(\alpha_2 + \mathrm{i}\beta_2)}$. Let $r_1 = \kappa_1 + \mathrm{i}\kappa_2$, $[(\alpha(4\mu^2 - \mathfrak{k}^2 + 2\mathfrak{c}^2) + \gamma \mathfrak{k}) + 2\mathrm{i}\mu(\alpha \mathfrak{k} - \gamma)] r_1 = \omega_1 + \mathrm{i}\omega_2$, then $r_2 = -(\kappa_1 + \mathrm{i}\kappa_2)$, $[(\alpha(4\mu^2 - \mathfrak{k}^2 + 2\mathfrak{c}^2) + \gamma \mathfrak{k}) + 2\mathrm{i}\mu(\alpha \mathfrak{k} - \gamma)] r_2 = -(\omega_1 + \mathrm{i}\omega_2)$. Here, α_i, κ_i and ω_i $(i = 1, 2)$ are the corresponding real and imaginary parts, respectively. Based on these facts, we can write (33) as

$$\Gamma = \frac{e^{\theta_1 + \mathrm{i}\theta_2} - e^{-(\theta_1 + \mathrm{i}\theta_2)}}{e^{\theta_1 + \mathrm{i}\theta_2 + \alpha_1 + \mathrm{i}\alpha_2} - e^{-(\theta_1 + \mathrm{i}\theta_2 + \alpha_1 + \mathrm{i}\alpha_2)}} e^{\mathrm{i}(\mathfrak{k} x + \omega)} \tag{34}$$

where

$$\theta_1 = \kappa_1 x + \omega_1 \tau, \qquad \theta_2 = \kappa_2 x + \omega_2 \tau.$$

Substituting (34) into (28), by a complicated computation, the breather solution of the Hirota equation (1) is derived

Table 4 The relationship between parameter μ and solutions' structures in (35)

μ	κ_1, κ_2	ω_1, ω_2	θ_1	θ_2	$\lvert\tilde{v}\rvert$
$\mu \in \Theta_1 \bigcap \Delta_1$	$\kappa_1 \neq 0,\ \kappa_2 = 0$	$\omega_1 = 0,\ \omega_2 \neq 0$	$\theta_1 = \kappa_1 x$	$\theta_2 = \omega_2 \tau$	KM
$\mu \in \Theta_1 \bigcap \Delta_2$	$\kappa_1 \neq 0,\ \kappa_2 = 0$	$\omega_1 \neq 0,\ \omega_2 = 0$	$\theta_1 = \kappa_1 x + \omega_1 \tau$	$\theta_2 = 0$	WS
$\mu \in \Theta_1 \cap C_{\mathbb{R}}(\Delta_1 \cup \Delta_2)$	$\kappa_1 \neq 0,\ \kappa_2 = 0$	$\omega_1 \neq 0,\ \omega_2 \neq 0$	$\theta_1 = \kappa_1 x + \omega_1 \tau$	$\theta_2 = \omega_2 \tau$	SB
$\mu \in \Theta_2 \bigcap \Delta_1$	$\kappa_1 = 0,\ \kappa_2 \neq 0$	$\omega_1 \neq 0,\ \omega_2 = 0$	$\theta_1 = \omega_1 \tau$,	$\theta_2 = \kappa_2 x$	AB
$\mu \in \Theta_2 \bigcap \Delta_2$	$\kappa_1 = 0,\ \kappa_2 \neq 0$	$\omega_1 = 0,\ \omega_2 \neq 0$	$\theta_1 = 0$	$\theta_2 = \kappa_2 x + \omega_2 \tau$	PS
$\mu \in \Theta_2 \cap C_{\mathbb{R}}(\Delta_1 \cup \Delta_2)$	$\kappa_1 = 0,\ \kappa_2 \neq 0$	$\omega_1 \neq 0,\ \omega_2 \neq 0$	$\theta_1 = \omega_1 \tau$	$\theta_2 = \kappa_2 x + \omega_2 \tau$	AB

The KM, WS, SB, AB, PS denote the time-periodic Kuznetsov–Ma breather, W-shaped soliton, spatiotemporally periodic breather, space-periodic Akhmediev breather and periodic solution

$$\tilde{v} = \left(1 + \frac{\frac{2(\mu+\mu^*)}{\mathfrak{c}} \frac{\sinh(\theta_1)\cos(\theta_2) + \mathrm{i}\cosh(\theta_1)\sin(\theta_2)}{\sinh(\theta_1+\alpha_1)\cos(\theta_2+\alpha_2) + \mathrm{i}\cosh(\theta_1+\alpha_1)\sin(\theta_2+\alpha_2)}}{1 + \frac{\cosh(2\theta_1) - \cos(2\theta_2)}{\cosh(2\theta_1+2\alpha_1) - \cos(2\theta_2+2\alpha_2)}} \right) \mathfrak{c} e^{\mathrm{i}(\mathfrak{k}x+\omega)}. \tag{35}$$

Obviously, the periodicity of solution (35) is mainly effected by θ_2. In a similar way as in the Sect. 3.2, we can get the time-periodic Kuznetsov–Ma breather, space-periodic Akhmediev breather, spatiotemporally periodic breather, W-shaped soliton and periodic solution for the Hirota equation (1). For the real parameters α, γ, $\mathfrak{c}$ and $\mathfrak{k}$, we define the following four sets:

$$\Theta_1 = \{\mu \in \mathbb{R} : \mu < -|\mathfrak{c}|, \mu > |\mathfrak{c}|\},$$
$$\Delta_1 = \left\{\mu \in \mathbb{R} : \alpha(4\mu^2 - \mathfrak{k}^2 + 2\mathfrak{c}^2) + \gamma\mathfrak{k} = 0\right\},$$
$$\Theta_2 = \{\mu \in \mathbb{R} : -|\mathfrak{c}| < \mu < |\mathfrak{c}|\},$$
$$\Delta_2 = \{\mu \in \mathbb{R} : \mu(\alpha\mathfrak{k} - \gamma) = 0\}.$$

Then, the relationship between parameters and solutions' structures in (35) for Eq. (1) is provided in Table 4.

Next, we are going to construct the continuum limit of the rogue wave solution from (24) with $k = 0$. By virtue of (26), (27) and (29), we obtain the corresponding continuum limit of Γ_n in (24) as

$$\Gamma = -\sigma_1 \left(1 + \frac{\sigma_2}{\sigma_1 \mathfrak{c} x + 4\sigma_1\sigma_2\mathfrak{c}^2(3\alpha\sigma_2\mathfrak{c} - \mathrm{i}\gamma\sigma_1)\tau - \sigma_2} \right) e^{-2\mathrm{i}\gamma\mathfrak{c}^2\tau}. \tag{36}$$

Inserting (36) into (28), through a tedious calculation, the rogue wave solution of the Hirota equation (1) is obtained

$$\tilde{v} = -\left(1 + \frac{16c^2\gamma\mathrm{i}\tau - 2}{32c^4(9\alpha^2c^2 + \gamma^2)\tau^2 + 2c^2x^2 + 48\alpha c^4\tau x - 2\sigma_1 cx - 24\alpha\sigma_1 c^3\tau + 1} \right) \mathfrak{c} e^{-2\mathrm{i}\gamma\mathfrak{c}^2\tau}. \tag{37}$$

As well known, different seed solutions to the same equation may lead to different new ones. Notice that the seed solution (30) is different from one in [40], so the breather solution (35) and the rogue wave solution (37) of Eq. (1) may be different from the ones given in [40]. Further, we can conclude that when $\mu^2 - \mathfrak{c}^2 \neq 0$, we are able to obtain the breather solutions for the Hirota equation (1), while $\mu^2 - \mathfrak{c}^2 = 0$, we can construct the rogue wave solution.

5 Conclusions

In this paper, the pseudopotential of the spatial discrete Hirota equation (3) is proposed for the first time, from which a Darboux–Bäcklund transformation (8) is constructed. Comparing it with the one-fold Darboux transformation obtained in [14], we find they are equivalent because there is no difference except for a constant times. And we believe this equivalence may hold universal if these two transformations are all derived from the same discrete spectral problem and using the similar technique in literatures [14] and [36,37], respectively. Various types of nonlinear wave solutions of Eq. (3), including bell-shaped one-soliton, three types of breathers, W-shaped soliton, periodic solution and rogue wave are given by using the obtained transformation (8), their evolutions and dynamical properties are illustrated graphically. Some important physical quantities such as amplitude, width, wave number, velocity, primary phase and energy of the bell-shaped one-soliton $|\tilde{u}_n|$ in (13) are listed in Table 1. Based on the nonlinear wave solution (23), the relationship between parameter λ and solutions' structures is presented in Tables 2 and 3. Finally, we show the continuum limit of breather and rogue wave solutions of the spatial discrete Hirota equation (3) yields the counterparts of the Hirota equation (1), and the relationship between parameter μ and solutions' structures is provided in Table 4. The method and technique used in this paper can also be applied to some other nonlinear integrable equations. The results in this paper might be useful for understanding some physical phenomena in nonlinear optics.

Acknowledgements The authors are very grateful to the editor and the anonymous referees for their valuable suggestions and hard work.

Author contributions F-CF derived Darboux–Bäcklund transformation, constructed various types of nonlinear wave solutions and established the continuum limit of breather and rogue wave solutions. All authors investigated the relationship between parameters and solutions' structures. F-CF wrote and revised the manuscript. S-YS and Z-GX helped to revise the manuscript. All authors gave final approval for publication.

Funding Funding This work is supported by National Natural Science Foundation of China (Grant Nos. 12271203 and 12201283), Natural Science Foundation of Fujian Province (Grant No. 2022J01892), Science and Technology Development Project of Jilin Province (Grant Nos. 20200201264JC and YDZJ202101ZYTS141), and the scientic research project of The Education Department of Jilin Province (Grant No. JJKH20220963KJ).

Data availibility The datasets generated during and/or analysed during the current study are available from the corresponding author on reasonable request.

Declarations

Conflict of interest The authors declare that there is no conflict of interests regarding the publication of this paper.

References

1. Hirota, R.: Exact envelope-soliton solutions of a nonlinear wave equation. J. Math. Phys. **14**, 805–809 (1973)
2. Mollenauer, L.F., Stolen, R.H., Gordon, J.P.: Experimental observation of picosecond pulse narrowing and solitons in optical fibers. Phys. Rev. Lett. **45**, 1095–1112 (1980)
3. Lakshmanan, M., Ganesan, S.: Equivalent forms of a generalized Hirota's equation with linear inhomogeneities. J. Phys. Soc. Jpn. **52**, 4031–4033 (1983)
4. Zhang, D.G., Liu, J.: A higher-order deformed Heisenberg spin equation as an exactly solvable dynamical equation. J. Phys. A: Math. Gen. **22**, L53–L54 (1989)
5. Sasa, N., Satsuma, J.: New-type of soliton solutions for a higher-order nonlinear Schrödinger equation. J. Phys. Soc. Jpn. **60**, 409–417 (1991)
6. Karpman, V.I., Rasmussen, J.J., Shagalov, A.G.: Dynamics of solitons and quasisolitons of the cubic third-order nonlinear Schrödinger equation. Phys. Rev. E **64**, 026614 (2001)
7. Ankiewicz, A., Soto-Crespo, J.M., Akhmediev, N.: Rogue waves and rational solutions of the Hirota equation. Phys. Rev. E **81**, 046602 (2010)
8. Porsezian, K., Lakshmanan, M.: Discretised Hirota equation, equivalent spin chain and Backlund transformations. Inverse Probl. **5**, L15–L19 (1989)
9. Narita, K.: Soliton solution for discrete Hirota equation. J. Phys. Soc. Jpn. **59**, 3528–3547 (1990)
10. Narita, K.: Soliton solution for discrete Hirota equation II. J. Phys. Soc. Jpn. **60**, 1497–5002 (1991)
11. Zhao, X.J., Guo, R., Hao, H.Q.: N-fold Darboux transformation and discrete soliton solutions for the discrete Hirota equation. Appl. Math. Lett. **75**, 114–120 (2018)
12. Ankiewicz, A., Akhmediev, N., Soto-Crespo, J.M.: Discrete rogue waves of the ablowitz-ladik and Hirota equations. Phys. Rev. E **82**, 026602 (2010)
13. Wen, X.Y., Wang, D.S.: Modulational instability and higher order-rogue wave solutions for the generalized discrete Hirota equation. Wave Motion **79**, 84–97 (2018)
14. Pickering, A., Zhao, H.Q., Zhu, Z.N.: On the continuum limit for a semidiscrete Hirota equation. Proc. R. Soc. A **472**, 20160628 (2016)
15. Yang, J., Zhu, Z.N.: Higher-order rogue wave solutions to a spatial discrete Hirota equation. Chin. Phys. Lett. **35**, 090201 (2018)
16. Li, M., Li, M.H., He, J.S.: Degenerate solutions for the spatial discrete Hirota equation. Nonlinear Dyn. **102**, 1825–1836 (2020)
17. Ma, L.Y., Zhang, Y.L., Zhao, H.Q., Zhu, Z.N.: Spatially discrete Hirota equation: rational and breather solution, gauge equivalence, and continuous limit. Commun. Nonlinear Sci. Numer. Simul. **108**, 106239 (2022)
18. Ablowitz, M.J., Clarkson, P.A.: Solitons, Nonlinear Evolution Equations and Inverse Scattering. Cambridge University Press, Cambridge (1991)
19. Hirota, R., Satsuma, J.: A variety of nonlinear network equations generated from the Bäcklund transformation for the Toda lattice. Prog. Theor. Phys. Suppl. **59**, 64–100 (1976)
20. Wazwaz, A.M., Kaur, L.: Complex simplified Hirota's forms and Lie symmetry analysis for multiple real and complex soliton solutions of the modified KdV-Sine-Gordon equation. Nonlinear Dyn. **95**, 2209–2215 (2019)
21. Ma, W.X.: N-soliton solutions and the Hirota conditions in (2+1)-dimensions. Opt. Quant. Electron. **52**, 511 (2020)
22. Geng, X.G., Dai, H.H., Cao, C.W.: Algebro-geometric constructions of the discrete Ablowitz–Ladik flows and applications. J. Math. Phys. **44**, 4573 (2003)

23. Wang, Z., Ma, W.X.: Discrete Jacobi sub-equation method for nonlinear differential–difference equations. Math. Methods Appl. Sci. **33**, 1463–1472 (2010)
24. Wen, X.Y.: Modulational instability and dynamics of multi-rogue wave solutions for the discrete Ablowitz–Ladik equation. J. Math. Phys. **59**, 073511 (2018)
25. Li, Q., Wang, D.S., Wen, X.Y., Zhuang, J.H.: An integrable lattice hierarchy based on Suris system: N-fold Darboux transformation and conservation laws. Nonlinear Dyn. **91**, 625–639 (2018)
26. Wang, H.T., Wen, X.Y.: Soliton elastic interactions and dynamical analysis of a reduced integrable nonlinear Schrödinger system on a triangular-lattice ribbon. Nonlinear Dyn. **100**, 1571–1587 (2020)
27. Fan, F.C., Shi, S.Y., Xu, Z.G.: Positive and negative integrable lattice hierarchies: conservation laws and N-fold Darboux transformations. Commun. Nonlinear Sci. Numer. Simul. **91**, 105453 (2020)
28. Fan, F.C.: Soliton interactions and conservation laws in a semi-discrete modified KdV equation. Chin. J. Phys. **71**, 458–465 (2021)
29. Guo, R., Zhao, H.H., Wang, Y.: A higher-order coupled nonlinear Schrödinger system: solitons, breathers, and rogue wave solutions. Nonlinear Dyn. **83**, 2475–2484 (2016)
30. Yu, F.J., Feng, S.: Explicit solution and Darboux transformation for a new discrete integrable soliton hierarchy with 4×4 Lax pairs. Math. Method Appl. Sci. **40**, 5515–5525 (2017)
31. Ma, W.X.: A Darboux transformation for the Volterra lattice equation. Anal. Math. Phys. **9**, 1711–1718 (2019)
32. Wang, M., Chen, Y.: Dynamic behaviors of mixed localized solutions for the three-component coupled Fokas–Lenells system. Nonlinear Dyn. **98**, 1781–1794 (2019)
33. Porsezian, K.: Bäcklund transformations and explicit solutions of certain inhomogeneous nonlinear Schrödinger-type equations. J. Phys. A: Math. Gen. **24**, L337–L343 (1991)
34. Sun, M.N., Deng, S.F., Chen, D.Y.: The Bäcklund transformation and novel solutions for the Toda lattice. Chaos Soliton. Fract. **23**, 1169–1175 (2005)
35. Pickering, A., Zhu, Z.N.: Darboux-bäcklund transformation and explicit solutions to a hybrid lattice of the relativistic toda lattice and the modified toda lattice. Phys. Lett. A **378**, 1510–1513 (2014)
36. Yang, Y.Q., Zhu, Y.J.: Darboux-Bäcklund transformation, breather and rogue wave solutions for Ablowitz–Ladik equation. Optik **217**, 164920 (2020)
37. Zhu, Y.J., Yang, Y.Q., Li, X.: Darboux-Bäcklund transformation, breather and rogue wave solutions for the discrete Hirota equation. Optik **236**, 166647 (2021)
38. Ma, L.Y., Zhao, H.Q., Shen, S.F., Ma, W.X.: Abundant exact solutions to the discrete complex mKdV equation by Darboux transformation. Commun. Nonlinear Sci. Numer. Simul. **68**, 31–40 (2019)
39. Zhao, H.Q., Yu, G.F.: Discrete rational and breather solution in the spatial discrete complex modified Korteweg-de Vries equation and continuous counterparts. Chaos **27**, 043113 (2017)
40. Tao, Y.S., He, J.S.: Multisolitons, breathers, and rogue waves for the Hirota equation generated by darboux transformation. Phys. Rev. E **85**, 026601 (2012)